


RESEARCH ARTICLE

Whole-exome sequencing revealed mutational profiles of giant cell glioblastomas

Zhi-feng Shi^{1*}; Kay Ka-Wai Li^{2,3*} ; Johnny Sheung Him Kwan²; Rui Ryan Yang²; Abudumijiti Aibaidula¹; Qisheng Tang¹; Yifeng Bao¹; Ying Mao¹; Hong Chen⁴; Ho-Keung Ng^{2,3}¹ Department of Neurosurgery, Huashan Hospital, Fudan University, Wulumuqi Zhong Road 12, Shanghai, 200040, China.² Department of Anatomical and Cellular Pathology, The Chinese University of Hong Kong, Prince of Wales Hospital, 30-32 Ngan Shing Street, Shatin, Hong Kong, China.³ Shenzhen Research Institute, The Chinese University of Hong Kong, No.10, 2nd Yuexing Road, Nanshan District, Shenzhen, 518057, China.⁴ Department of Pathology, Huashan Hospital, Fudan University, Wulumuqi Zhong Road 12, Shanghai, 200040, China.**Keywords**

giant cell glioblastoma, hypermutation phenotype, whole-exome sequencing.

Corresponding author

Hong Chen, Department of Pathology, Huashan Hospital, Fudan University, Wulumuqi Zhong Road 12, Shanghai 200040, China. Email: cherrychen30@126.com

Ho-Keung Ng, Department of Anatomical and Cellular Pathology, The Chinese University of Hong Kong, Hong Kong. Email: hkng@cuhk.edu.hk

Received 11 December 2018

Accepted 4 March 2019

Published Online Article Accepted 12 March 2019

*Authors contributed equally to this work.

doi:10.1111/bpa.12720

Abstract

Giant cell glioblastoma (gcGBM) is a rare histological variant of GBM, accounting for about 1% of all GBM. The prognosis is poor generally though gcGBM does slightly better than the other IDH-wild-type GBM. Because of the rarity of the cases, there has been no comprehensive molecular analysis of gcGBM. Previously, single-gene study identified genetic changes in TP53, PTEN and TERT promoter mutation in gcGBM. In this report, we performed whole-exome sequencing (WES) to identify somatically acquired mutations and copy number variations (CNVs) in 10 gcGBM genomes. We also examined TERT promoter mutation and MGMT methylation in our cohort. On top of the reported mutations, WES revealed ATRX, PIK3R1, RB1 and SETD2 as the recurrent mutations in gcGBM. Notably, one tumor harbored a mutation in MutS homolog 6 (MSH6) that is a key mismatch repair (MMR) gene. This tumor demonstrated hypermutation phenotype and showed an increased number of somatic mutations. TERT promoter mutation and MGMT methylation were observed in 20% and 40% of our samples, respectively. In conclusion, we described relevant mutation profiling for developing future targeted therapies in gcGBM.

INTRODUCTION

Giant cell glioblastoma (gcGBM) is a rare histological variant of GBM that constitutes approximately 1% of all GBM (22, 35). Histologically, gcGBM is characterized by numerous bizarre, multinucleated giant cells as large as 0.5 mm in diameter with astrocytic differentiation (22, 37). Compared to regular GBM, gcGBM is more often present in younger patients (35). Despite the poor prognosis for GBM, this variant is associated with improved clinical outcome compared to the regular IDH-wild-type GBM (24, 38, 42). At present, the best treatment strategy of gcGBM has not yet been ascertained. Like GBM, complete surgical resection, radiation and chemotherapy are the mainstay of gcGBM management.

The underlying genetic alterations caused gcGBM remain obscure because of scarcity of samples for molecular examination and the low incidence of the disease. TP53

mutation is common in gcGBM and was identified in about 80% of tumors using first-generation sequencing approach (30, 32). Mutations in PTEN and TERT promoter were also found in gcGBM to a lesser extent (34, 39). Similar to primary GBM, gcGBM often do not carry IDH mutation (25, 56). At chromosomal level, 50% and 42% of gcGBM showed loss of chromosome 10q and 19q, respectively (34). However, frequent EGFR amplification detected in regular GBM is only observed in less than 10% of gcGBM (30, 32).

Advancement in high-throughput next-generation sequencing allows oncologists to decipher genomic landscape of tumors. We conducted whole-exome sequencing (WES) of 10 gcGBM samples and matched blood. The goals of this study were to sequence the exome of gcGBM to identify potentially recurrent somatic mutations and copy number variations (CNVs) in gcGBM.

MATERIALS AND METHODS

Frozen tissue specimens

A total of 10 primary, treatment-naïve giant cell GBMs were obtained at the time of neuro-oncology service between years 2010 and 2015 at Huashan Hospital, Shanghai. Tissues were snap frozen and stored at -80°C until use. Samples were histologically reviewed by two neuro-pathologists (Ng HK and Chen H) and diagnosed according to WHO 2016. Clinicopathological information of the patients is summarized in Table 1. This study was approved by the Ethics Committee of Huashan Hospital, Fudan University.

Whole-exome sequencing

DNA was extracted from tissue and blood using Qiagen DNAeasy kits (Qiagen). DNA was quantified using Nanodrop ND-100 (Thermo Scientific, Waltham, MA) and Qubit 2.0 Fluorometer (Life Technologies, Carlsbad, CA, USA). Library preparation, exome capture and sequencing were done by Genetron Health (Shanghai, China). Genomic DNA were captured and amplified with Agilent Technologies SureSelect Human All Exon version 5 (Agilent Technologies, Santa Clara, CA, USA), followed by paired-end sequencing on HiSeq2500 platform (Illumina Inc., San Diego, CA, USA). The raw data of WES are available upon request.

Data analysis

Sequencing reads were mapped to the human genome (GRCh37) using Burrows-Wheeler Alignment tool (BWA). Duplicate reads were then marked using Picard (<http://broadinstitute.github.io/picard/>), and mapped reads around known deletions were locally realigned using Genome Analysis Toolkit (GATK) to improve the overall quality of alignment.

Single nucleotide variants (SNVs) and short insertions and deletions (indels) were detected using MuTect2 (10) and Strelka (43), and their functional effects were annotated using ANNOVAR (52). Potential germline mutations were removed if a mutation had a frequency of greater

than 1% in public databases (ExAC, ESP and 1000 Genomes Project). Copy number variations were interrogated with CNVkit (49). GISTIC version 2.0 (<http://archive.broadinstitute.org/cancer/cga/gistic>) analysis was performed to identify significantly recurrent copy number gains and losses at focal level, defined as regions spanning $<50\%$ of a chromosome arm. A \log_2 ratio above 0.3 was considered as “gain,” and a \log_2 ratio below -0.3 was considered as “loss.” Amplification and homozygous loss were considered when \log_2 ratio was >2.0 and <2.0 , respectively.

Pathway and GO enrichment analyses

ConsensusPathDB of the Max Planck Institute for Molecular Genetics was used in pathway and GO enrichment analyses (16). We searched for pathways as defined KEGG, with a minimum of 5% members and a Q -value cutoff at 0.05. Also, we performed an enrichment analysis based on Gene Ontology Biological Process Level 5 with the same website and analysis tool, and a Q -value of <0.05 was regarded as significant.

TERT promoter mutation analysis

PCR amplification was conducted on DNA extracted from formalin-fixed, paraffin-embedded (FFPE) tissues. The primer sequences were 5'-GTCCTGCCCTTCACCTT-3' and 5'-CAGCGCTGCCTGAAACTC-3', and amplified a 163-bp fragment with KAPA2G Robust HotStart ReadyMix (Sigma). The PCR product was purified and sequenced with BigDye Terminator Cycle Sequencing kit v1.1 (Life Technologies). The products were resolved in 3130xl Genetic Analysis.

O6-methylguanine-DNA methyltransferase (MGMT) methylation analysis

MGMT methylation status was evaluated by methylation-specific polymerase chain reaction (MSP) according to our previous report (11).

Table 1. Patient characteristics of 10 giant cell glioblastomas in this study.

Patient	Age	Sex	KPS score at diagnosis	Survival status	Overall survival (months)	Chemotherapy (yes/no)	Radiotherapy (yes/no)	Extent of resection (total vs non-total)
1	39	F	70	Dead	10.37	Yes	Yes	Total
2	17	M	90	Dead	11.50	Yes	Yes	Total
3	39	F	80	Dead	12.67	Yes	Yes	Total
4	12	F	90	Dead	12.93	Yes	Yes	Total
5	42	M	80	Dead	13.23	Yes	Yes	Total
6	41	M	90	Dead	27.16	Yes	Yes	Total
7	50	F	90	Dead	28.00	Yes	Yes	Total
8	30	F	80	Alive	35.16	Yes	Yes	Total
9	63	M	80	Alive	36.70	Yes	Yes	Total
10	51	F	80	Alive	38.00	Yes	Yes	Total

RESULTS

Clinical characteristic of 10 gcGBM

To explore the mutational profiling in gcGBM, we performed WES on 10 primary, treatment-naïve gcGBM tumors

and matched blood samples. The mean and median ages of the samples were 38.4 and 40 years old, respectively. This is consistent with the literature that gcGBM is present in younger population compared to classical GBM (33, 35). Male and female ratio was 1:1.5. All tumors were found in the hemisphere with majority of them (70%; 7/10)

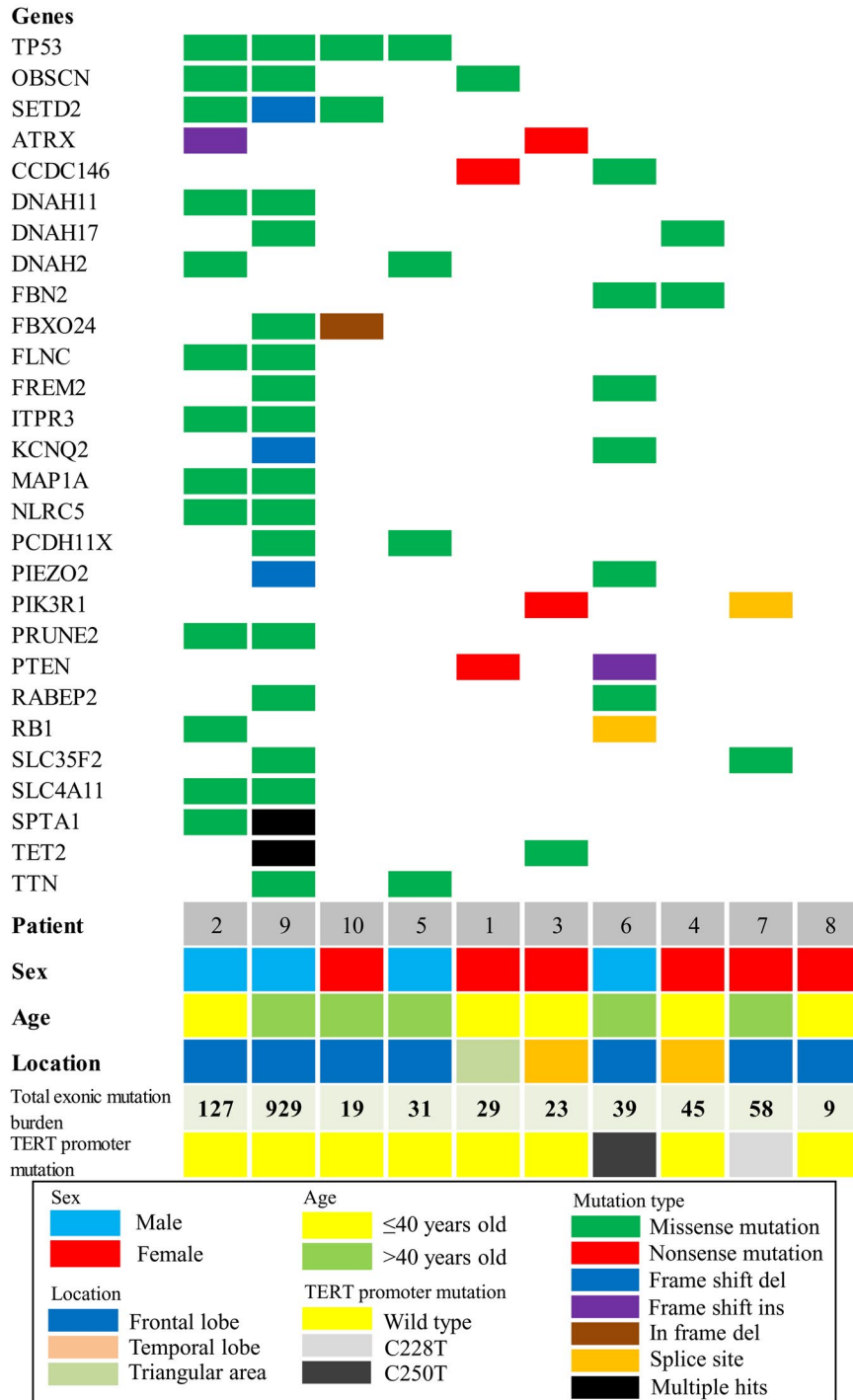


Figure 1. Mutation spectrum of giant cell glioblastomas. The heat map illustrates recurrent mutations found in 10 gcGBM samples. Type of mutation is represented by different colors. The bottom indicates age,

sex, tumor location, number of mutations and TERT promoter mutation status of individual samples.

located in the frontal lobe (Table 1). Tumors located in the temporal lobe were found in two cases. All patients had undergone surgery, chemotherapy and radiotherapy. Histology of all cases can be found in Supporting Information Figure S1.

Mutational spectrum in gcGBM

The mean coverage was $75.19 \times$ for gcGBM and $85.97 \times$ for normal samples. A total of 1312 tumor-specific (somatic) mutations were identified, of which 947 were non-silent. Interestingly, our cohort has a median of 35 coding mutations per tumor, which is about 2 times lower compared to regular GBM (29). Excluding the hypermutated tumor which will be discussed below, the nine samples had a median rate of 0.62 coding mutations per megabase, which is 3.5-fold lower compared to regular GBM (4).

We found 28 recurrent mutations (Figure 1; Supporting Information Table S1). TP53 mutation was present in 4 of 10 tumors, representing the most frequent genomic

alteration in our sample set. The result is in concordance with previous literature showing high frequency of TP53 mutation in gcGBM (32, 39). Notably, mutation in ATRX, PIK3R1, RB1 and SETD2 was identified in 20%, 20%, 20% and 30% of gcGBM, respectively. These gene mutations have not been reported in gcGBM, albeit in low- and high-grade gliomas (8, 13, 55). We also identified PTEN mutation in 20% of gcGBM, and the incidence is in agreement with the literature (32, 39). We did validate the mutations identified in gcGBMs by Sanger sequencing. Examples are shown in Figures 2–4.

Pathway analysis revealed that the 28 recurrent alterations found in our exome study were significantly (i.e., $FDR Q\text{-value} < 0.05$) enriched with 3 pathways in KEGG. As shown in Table 2, they were “Glioma—Homo sapiens (human)” ($FDR Q\text{-value} = 3.15 \times 10^{-5}$), “Melanoma—Homo sapiens (human)” ($FDR Q\text{-value} = 3.15 \times 10^{-5}$) and “Endometrial cancer—Homo sapiens (human)” ($FDR Q\text{-value} = 2.59 \times 10^{-4}$). The recurrent alterations contained in the last two pathways are essentially subsets of those

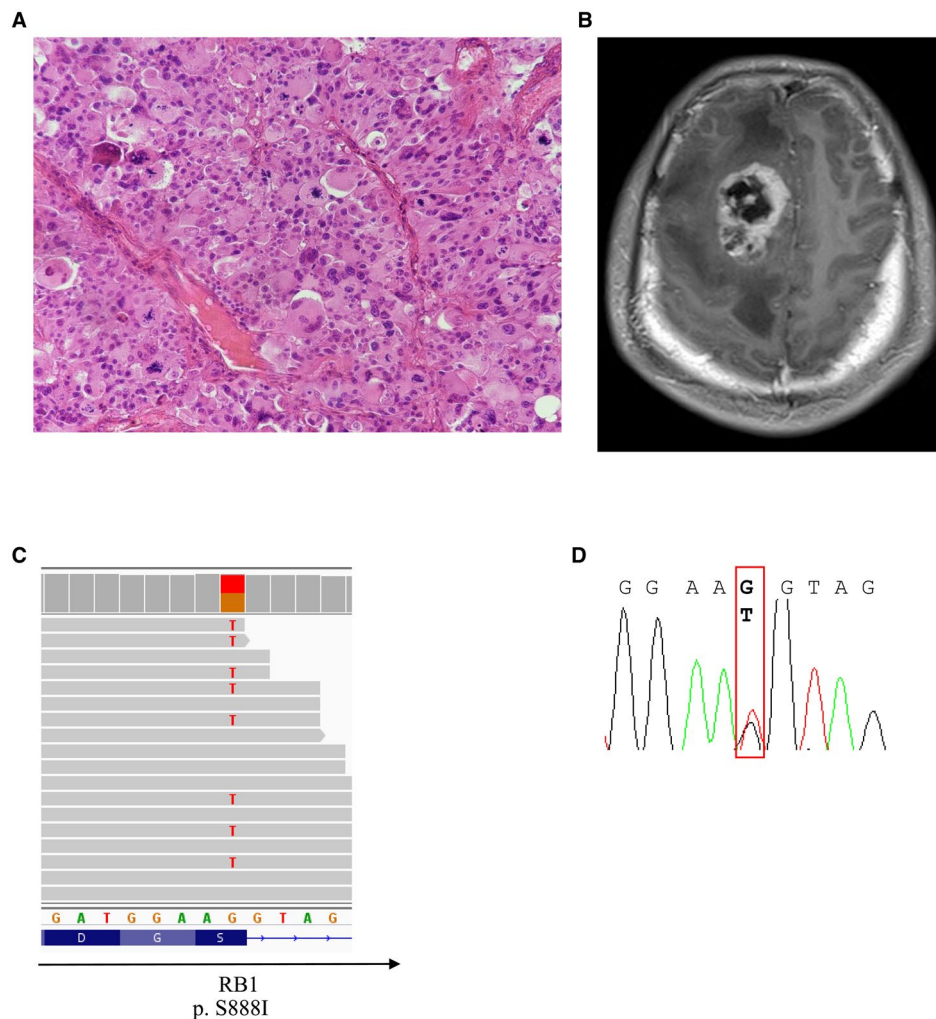


Figure 2. Histology and radiologic feature of a gcGBM from a 17-year-old male with *RB1* mutation. A. H&E section of the tumor and B. T1-enhanced MRI of the tumor mass. C. Integrative Genomics Viewer

(IGV) screenshot illustrates *RB1* mutation. D. *RB1* mutation was confirmed by Sanger sequencing.

contained in the glioma pathway. Gene ontology analysis of the 28 recurrent alternations identified “GO:0034349-gliial cell apoptotic process” as the only significantly enriched term from the GO Biological Process Level 5 (FDR Q -value = 1.68×10^{-2} ; Table 3).

Copy number variations

CNVs were determined using software package CNVKit, which analyzed copy number based on read depth in the on-target and off-target reads (49). As shown in Figure 5, arm-level copy number variation was identified in all patients except patients 8 and 10. Recurrent arm-level gains were found at chromosomes 7 ($n = 6$) and 20 ($n = 2$). Recurrent arm-level losses were occurred at chromosomes 10q ($n = 2$) and 22q ($n = 2$). One case displayed loss of the long arm of chromosome 10 (10q) also carried a PTEN mutation.

We then conducted GISTIC analysis to determine statistically significant recurrent focal gains and losses. As

shown in Figure 6 and Table 4, we found in the gcGBM genome eight significantly focal loss regions including 6p21.32, 7q34, 8p11.22, 14q32.33, 19q13.42, 22q11.23 and 22q13.1. Genes located in these regions include ADAM3A, APOBEC3A, GSTT1, HLA-DRB6, JAG2, KIR2DL1, KIR2DL3, KIR2DL4, LINC00226, LINC00221 and PRSS3P2. No recurrent focal gains were found in this cohort. We did detect a gcGBM from a 50-year-old female patient harboring amplifications for EGFR, MDM2 and CDK4. Neither EGFR, MDM2 nor CDK4 amplification was detected in the other nine samples. Thus, these aberrations did not reach significance in GISTIC analysis.

A hypermutation phenotype and somatic MSH6 mutation in gcGBM

We found one gcGBM harbored high number of somatic exonic mutations (Figures 1 and 4). This tumor had 929

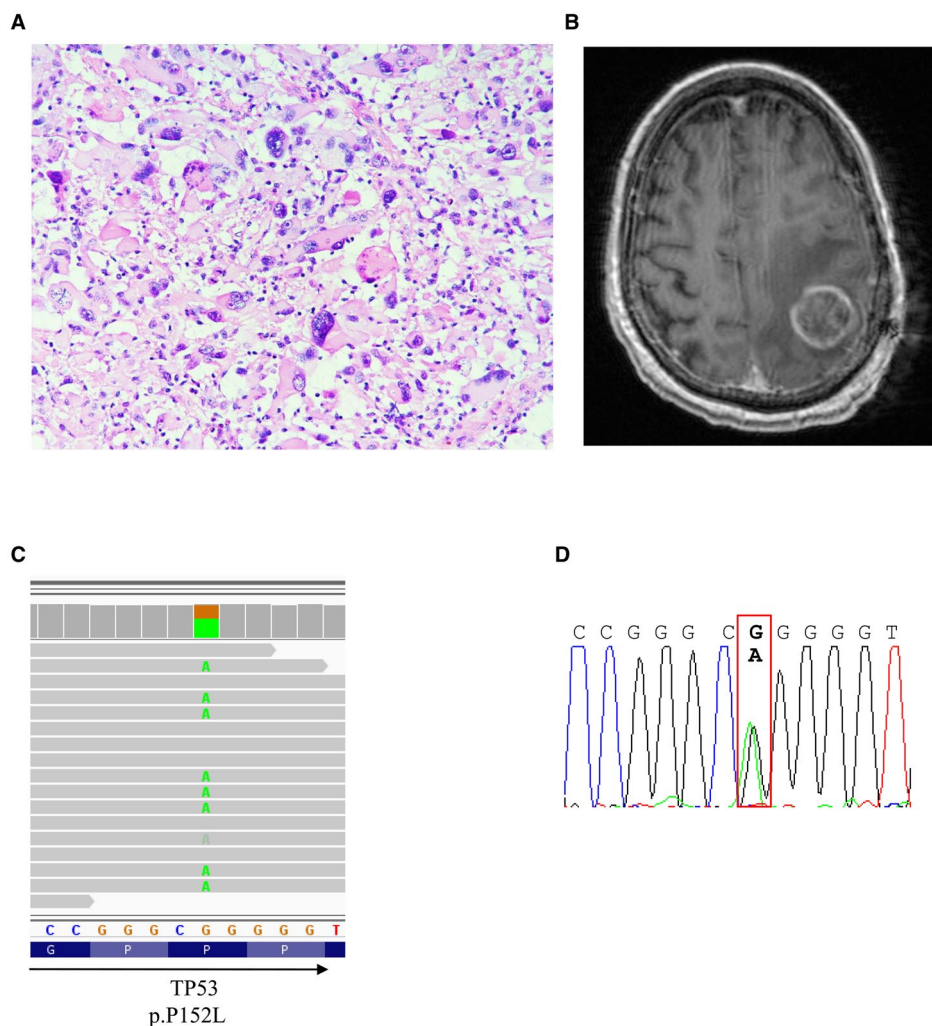


Figure 3. Histology and radiologic feature of a gcGBM from a 42-year-old male with TP53 mutation. A. H&E section and B. T1-enhanced images of the tumor. C. TP53 mutation was visualized with IGV and D. validated by Sanger sequencing.

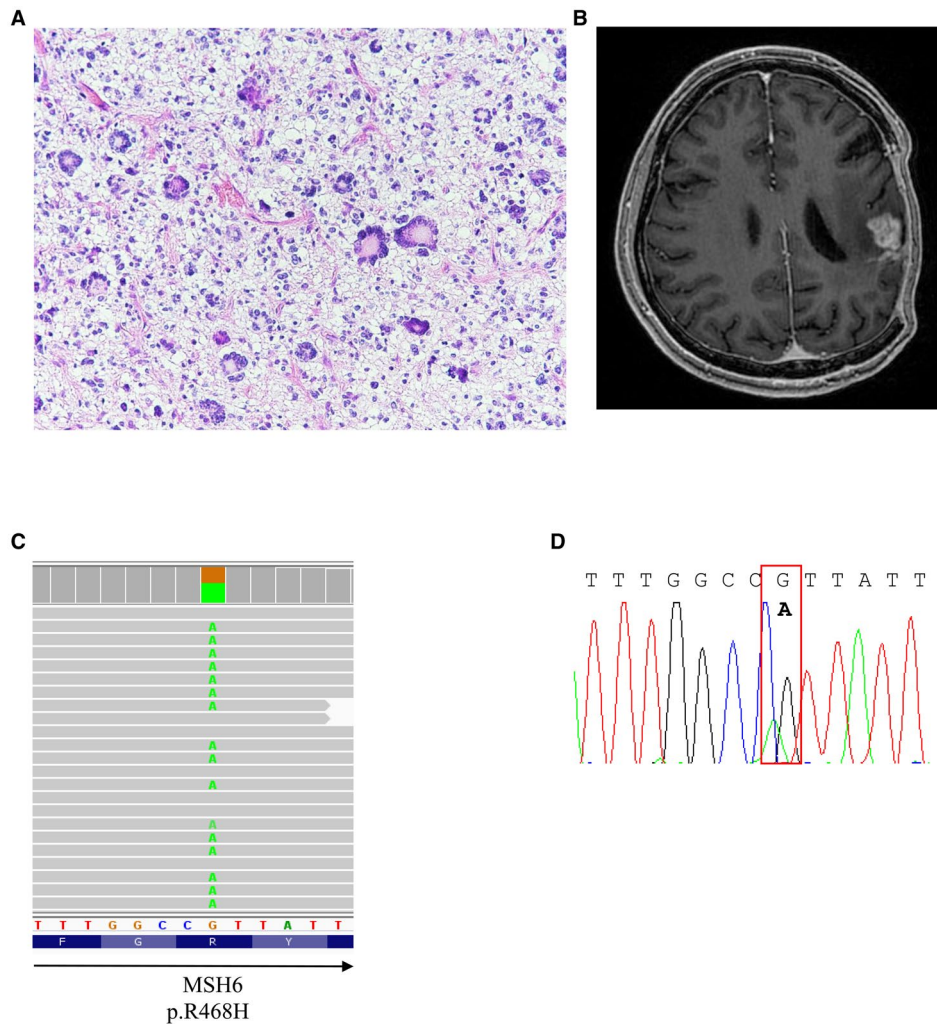


Figure 4. Representative figures of H&E and MRI imaging of a 63-year-old gcGBM possessing MSH6 mutation. A. H&E section and B. T1-enhanced images of the tumor. C. The missense mutation was visualized with IGV and D. confirmed by Sanger sequencing.

somatic mutations which is equivalent to 18.46 exonic mutation/Mb, representing a rate 22 times greater, on average, than the rate found in the other 9 cases.

The tumor with high number of somatic mutations carried a mutation in MutS homolog 6 (MSH6), resulting a change of amino acid from arginine (R) to histidine (H) at residue 468 at location inside the MutS domain I involved in DNA binding. Mutation at this position has been identified in prostate and stomach cancers (17, 41). In The Cancer Genome Atlas (TCGA) GBM study, MSH6 mutation was identified in 1.1% of tumors, and 2/3 of the mutations were located outside of MutS domain I.

TERT promoter mutation in gcGBM

TERT promoter mutation was identified in 2/10 (20%) samples. One sample carried C228T mutation, and another sample had C250T. The ages of these tumors were 41 and 50 years old, and the overall survival of them was

Table 2. Pathway analysis of 28 recurrent mutations in giant cell glioblastoma.

KEGG pathways	Recurrent alterations	P-value	FDR Q-value
Glioma—Homo sapiens (human)	PIK3R1, RB1, PTEN, TP53	2.98×10^{-6}	3.15×10^{-5}
Melanoma—Homo sapiens (human)	PIK3R1, RB1, PTEN, TP53	3.15×10^{-6}	3.15×10^{-5}
Endometrial cancer—Homo sapiens (human)	PIK3R1, PTEN, TP53	7.78×10^{-5}	2.59×10^{-4}

Only significant (Q -value < 0.05) pathways from KEGG with at least 5% members containing recurrent alterations are shown.

27–28 months. The mutation frequency in this study was similar to that in Oh *et al* study showing TERT promoter mutation in one-quarter of gcGBM (34).

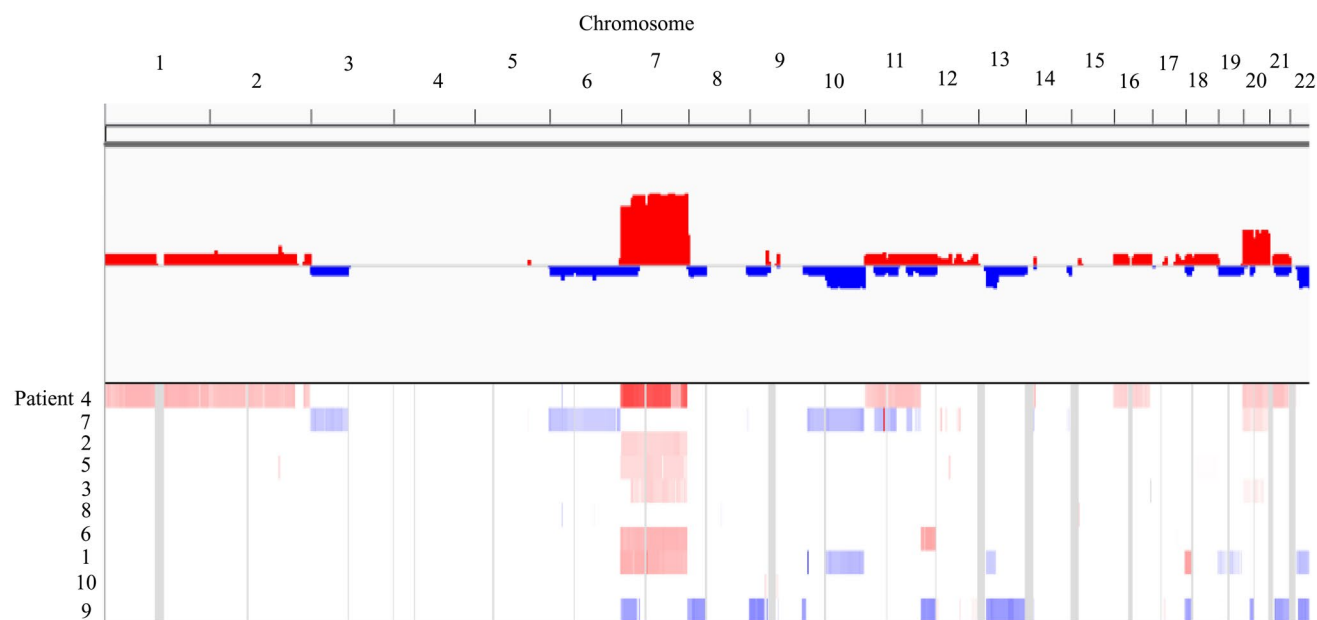


Figure 5. Arm-level copy number variations in gcGBM. Chromosome gains (shown in red) and losses (shown in blue) were identified by WES. The numbers on top of the plot represent chromosome number (1–22), and the numbers on the left indicate patient number.

MGMT methylation status in gcGBM

Four gcGBM samples (40%) were positive for MGMT methylation as revealed by MSP. Similar prevalence of MGMT methylation was reported by Lohkamp *et al* (28). MGMT methylation was not associated with age, sex or overall survival.

DISCUSSION

Giant cell glioblastoma (gcGBM) is a very rare disease and occurs in approximately 1% of all GBM (24, 38, 39, 44). Because of uncommon nature of this tumor entity, very few studies have reported the genomic and genetic alterations underlying this disease. We here employed next-generation sequencing approach to reveal genomic-wide mutational landscape of this entity, and identified potential-mutated genes for target therapy.

First, we described the tumor mutation rate in gcGBM is much lower than the rates observed in regular GBM and other cancers (4, 29). Then, we found TP53 is the most frequent mutated gene in gcGBM, accounting for 40% of our cohort. The result is concordant with previous report showing the high prevalence of p53 mutation in gcGBM (30–32). TP53 is a well-known tumor suppressor that is involved in cell cycle regulation and is dysregulated in 30% of primary de novo GBM and 65% of secondary GBM (36). Previous studies indicated nearly 80% of GBM had dysregulated p14^{ARF}/MDM2/p53 pathway either by p53 mutation, amplification of MDM2 or deletion/mutation of p14^{ARF} (19). In our cohort, amplification of MDM2 was found in one case, and this sample carried the wild-type

TP53 (see discussion). Deletion of p14ARF was identified in one case and the tumor had a mutation in TP53 gene. Mutation of p14ARF was not found in our cohort. Thus, 50% of our cohort (case #2, #5, #7, #9 and #10) showed p53 mutation, MDM2 amplification or p14ARF deletion. Besides TP53, RB1 (chromosome 13q14) is another well-known tumor suppressor that also controls progression through G1 into the S-phase of the cell cycle. Aberration of RB1 is found in around 10% of GBM according to TCGA (4). In this study, two gcGBM samples (20%) harbored RB1 mutation and one of them also carried a mutation in TP53 gene. Although we found RB1 mutation at a rate higher than in regular GBM, we have to be cautious in interpreting the data with our small sample size.

PTEN and PIK3R1 are members of RTK/RAS/PI(3)K signaling pathway, that plays key roles in proliferation, differentiation and survival of cancer cells. Nearly 90% of the regular GBMs showed various alterations leading to an aberrant activation of RTK/RAS/PI(3)K signaling cascade (8). In this study, we found 20% of gcGBM-harbored PTEN mutation. The prevalence is consistent with the literature (39). PIK3R1 encodes a regulatory protein p85 α , that forms the PI(3)K complex with a catalytically active protein p110 α , and it is mutated in ~10% of the regular GBMs according to TCGA (8). We found two samples (20%) of gcGBM-harbored PIK3R1 mutation, and one of them also had copy number gain in PIK3R1. PTEN and PIK3R1 mutations were mutually exclusive in this study and they did not overlap with TP53 mutation. Collectively, they made up of 40% of our cohort (case #1, #3, #6 and #7; Figure 1). We speculated that these tumors showed activation of RTK/RAS/PI(3)K signaling pathway. Further

Table 3. Gene Ontology (GO) terms associated with recurrent mutations in giant cell glioblastoma.

GO term ID	Biological process description	Recurrent alterations	P-value	FDR Q-value
GO:0034349	Glial cell apoptotic process	RB1, TP53	1.84×10^{-4}	1.68×10^{-2}

Only significant (Q -value < 0.05) terms from the GO Biological Process Level 5 with at least 5% members containing recurrent alterations are shown.

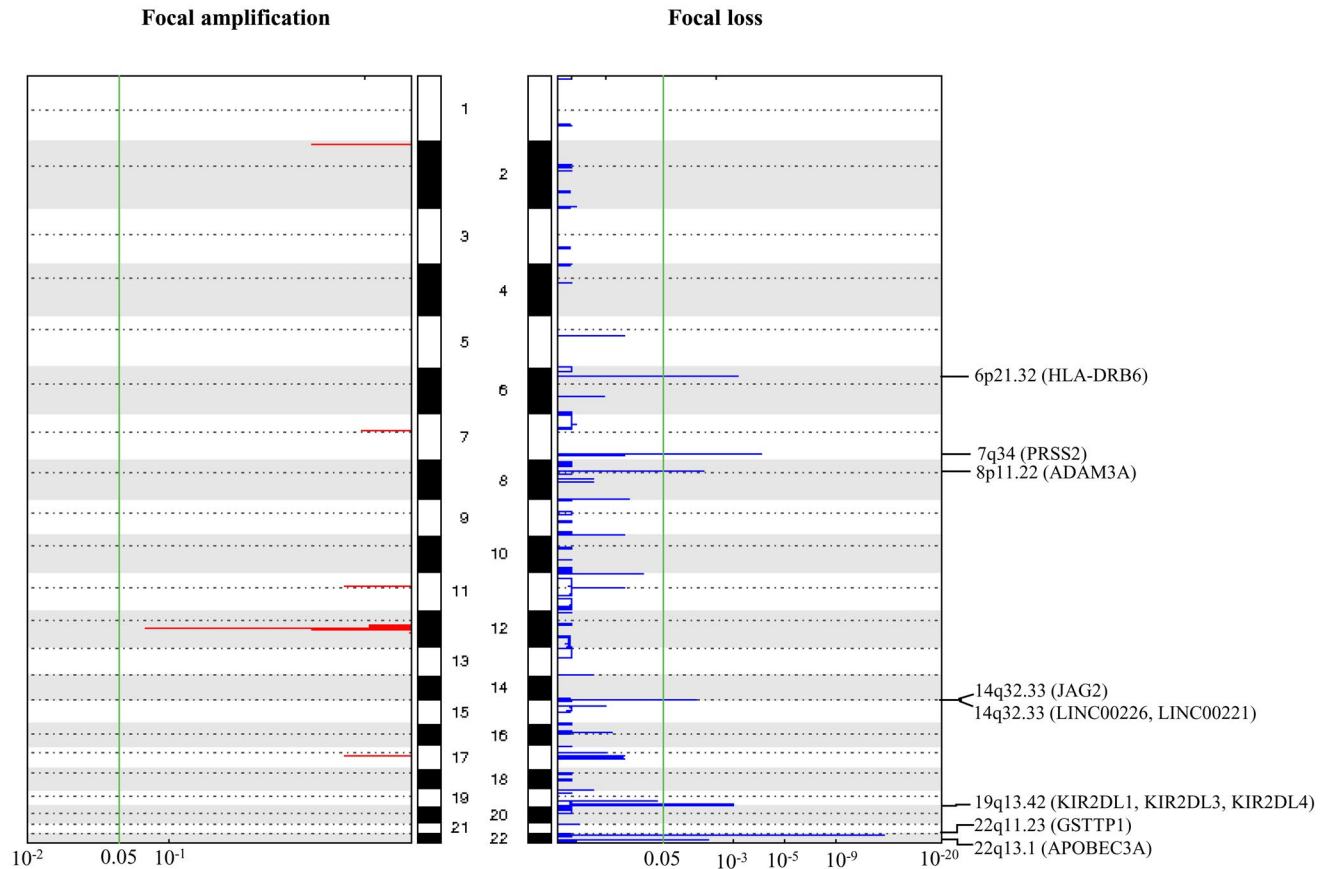


Figure 6. Significant focal copy number variations in gcGBM as revealed by GISTIC 2.0. The plot illustrates the statistical significance of aberrations displayed as FDR Q-values (x-axes). The human chromosomes 1 to 22 (hg19) are indicated along the y axis. Eight focal regions surpass the significance threshold (green line). Chromosomal

locations of GSTT1, PRSS2, HLA-DRB6, KIR2DL1, KIR2DL3, KIR2DL4, APOBEC3A, ADAM3A, JAG2, LINC00226 and LINC00221 Q-value are indicated on the plot.

studies are required to verify the role of this pathway in the pathogenesis of gcGBM.

Furthermore, we reported for the first time recurrent mutation in ATRX and SETD2 in gcGBM. Mutation in ATRX (alpha thalassemia/mental retardation syndrome X-linked), a SWI2/SNF2 family of DNA helicases functioned in chromatin modulation and maintenance of telomeres, is known in pediatric and adult gliomas (23), but has not been reported in gcGBM. Mutation in ATRX leads to epigenetic alterations, and epigenetic alteration is known to play a role in tumorigenesis (14, 20). In astrocytic tumors, DNA methylation profile was different between tumors with low- and high-ATRX expression (6). Thus, it is

possible that ATRX mutation could lead to alterations in global genomic methylation and gene expression in gcGBM. The gene SETD2 (KMT3A) is located on chromosome 3p21.31, and it encodes a methyltransferase that mediates trimethylation of H3K36 (H3K36me3). SETD2 is also involved in chromatin organization (48). Mutation of SETD2 is often described in pediatric high-grade gliomas (PHGG) and many other tumors, including kidney, lung and liver cancers (9, 13, 26). In PHGG, SETD2 mutation leads to disruption of trimethyltransferase activity and distinct global DNA methylation signature (9, 13, 48). Recent study further demonstrated that SETD2 mutation is present in low- and high-grade gliomas of children and adults and of

Table 4. Focal copy number variations in giant cell glioblastoma.

Cytoband	FDR Q-value	Peak boundaries	Genes
22q11.23	5.27×10^{-13}	chr22:24325343-24373954	GSTTP1
7q34	9.48×10^{-5}	chr7:142470509-142482020	PRSS2
6p21.32	7.04×10^{-4}	chr6:32497787-32546606	HLA-DRB6
19q13.42	1.02×10^{-3}	chr19:55241149-55331354	KIR2DL1, KIR2DL3, KIR2DL4
22q13.1	5.18×10^{-3}	chr22:39338026-39369501	APOBEC3A
8p11.22	6.59×10^{-3}	chr8:39254268-39427923	ADAM3A
14q32.33	1.07×10^{-2}	chr14:105525907-105644252	JAG2
14q32.33	1.15×10^{-2}	chr14:106436558-107349540	LINC00226, LINC00221

hemisphere and midline (51). SETD2 mutation in gliomas was also associated with decreased H3K36me3 expression (13, 51). We further examined SETD2 and H3K36me3 levels by immunohistochemistry in our cohort. We adopted a semiquantitative scoring system in which signal intensity and percentage of positive cells were considered as parameters in grading IHC staining result (27). We found SETD2 expression level was not significantly different between SETD2-wild-type and SETD2-mutant tumors. Yet, H3K36me3 level (determined by antibody Abcam ab9050) was significantly lower in the three SETD2-mutant gcGBMs [0.33 ± 0.577 (mean \pm SD)] compared to the wild-type gcGBMs [4.43 ± 2.936 (mean \pm SD); $P = 0.049$; Supporting Information Figure S2]. Our results suggested SETD2 mutations lead to a decrease in H3K36me3 expression in gcGBM.

Aside from ATRX, PIK3R1, RB1 and SETD2, we detected OBSCN mutation in 30% (3/10) of gcGBM. The patients were aged 17–63. Copy number variation in MYCN was seen in one patient (#1) and arm-level copy number variation in chromosome 22q was observed in two patients (#1 and #9; Figure 5). None of these variations was found in non-OBSCN mutant tumors. The gene OBSCN is located on chromosome 1q42.13. It encodes obscurins which are large cytoskeletal proteins with structural and regulatory roles (40). OBSCN is highly mutated in cancers and the mutation has been found in melanoma, salivary gland carcinoma, pancreatic, breast and colorectal cancers (2, 21, 47). Reduced obscurins expression level has been reported in breast cancer and depletion of obscurins leads to disruption of cell-cell contacts and acquisition of a mesenchymal phenotype that leads to enhanced tumorigenesis, migration and invasiveness (46). In colorectal carcinoma, OBSCN mutation was found early in carcinogenesis and was considered an early driver of carcinogenesis (54). In contrast, OBSCN was not considered as a cancer driver gene in another study (50).

We then did a pathway analysis with ConsensusPathDB (16) and found that the glioma pathway in KEGG (involving TP53, PTEN, RB1 and PIK3R1 among the 28 recurrent alternations) was altered in 70% of cases (FDR Q -value = 3.15×10^{-5}). Gene ontology analysis suggested that 7.1% of these recurrent mutations (i.e., RB1, TP53) were related to glial cell apoptotic process (FDR Q -value = 1.68×10^{-2}).

Furthermore, we explored CNVs in our cohort. At arm-level, we showed that gain of chromosome 7 was the most

frequent CNV, followed by gain of chromosome 20 and losses of 10q and 22q. EGFR is located on chromosome 7, and is amplified in >40% of regular GBM. However, such alteration is less frequently detected (<10%) in gcGBM (38). We detected EGFR amplification in only one gcGBM (10%) diagnosed at the age of 50. Interesting, the same patient had MDM2 and CDK4 amplifications, and no other patient in this cohort showed EGFR, MDM2 or CDK4 amplification.

At focal level, we identified eight highly recurrent loss regions in gcGBM. All of them had at least one gene located within the focal loss regions. For instance, the focal loss region on chromosome 14q32.33 contains the gene JAG2, which encodes one of the four transmembrane ligands that bind to NOTCH receptors (12). The binding of ligand to NOTCH receptors induces cleavage of receptor, releases NOTCH intracellular domain and activates NOTCH target genes. Another focal loss region located on chromosome 8p11.22 involves the gene ADAM3A, which is deleted in 16% of pediatric high-grade gliomas (3). We also identified a focal loss at chromosome 14q32 which contains a long noncoding RNA LINC00226 that was downregulated in pancreatic ductal adenocarcinoma (58).

Here, we also reported a single case of primary gcGBM exhibited hypermutated phenotype. This tumor carried a missense mutation at amino acid residue 468 of the MSH6 gene. High frequency of hypermutation has been identified in melanoma, bladder and lung cancer (1, 15, 53). Hypermutation has also been identified in pediatric and adult brain tumors (7, 45). The gene MSH6 is located on chromosome 2p16.3, and it is a main player in DNA mismatch repair system (MMR). Hypermutation phenotype has been linked to MSH6 mutation in GBM after alkylating agent or temozolomide treatment (5, 18). In fact, all four MSH6 mutations found in GBM by TCGA were posttreatment samples, and subsequent study showed absent of MSH6 mutation in the matched treatment-naïve biopsies (57).

In conclusion, by next-generation sequencing, we have identified potential clinically relevant mutations for targeted therapy in gcGBM.

ACKNOWLEDGMENTS

This study was supported by National Natural Science Foundation of China (NSFC, grant numbers 81472373 and

81702471), and Shenzhen Science Technology and Innovation Commission (reference number JCYJ20170307165432612).

CONFLICT OF INTEREST

The authors have no conflict of interest.

REFERENCES

- Akbani R, Akdemir KC, Aksoy BA, Albert M, Ally A, Amin SB *et al* (2015) Cancer Genome Atlas Network. Genomic classification of cutaneous melanoma. *Cell* **161**:1681–1696.
- Balakrishnan A, Bleeker FE, Lamba S, Rodolfo M, Daniotti M, Scarpa A *et al* (2007) Novel somatic and germline mutations in cancer candidate genes in glioblastoma, melanoma, and pancreatic carcinoma. *Cancer Res* **67**:3545–3550.
- Barrow J, Adamowicz-Brice M, Cartmill M, MacArthur D, Lowe J, Robson K *et al* (2011) Homozygous loss of ADAM3A revealed by genome-wide analysis of pediatric high-grade glioma and diffuse intrinsic pontine gliomas. *Neuro Oncol* **13**:212–222.
- Brennan CW, Verhaak RG, McKenna A, Campos B, Noushmehr H, Salama SR *et al* (2013) The somatic genomic landscape of glioblastoma. *Cell* **155**:462–477.
- Cahill DP, Levine KK, Betensky RA, Codd PJ, Romany CA, Reavie LB *et al* (2007) Loss of the mismatch repair protein MSH6 in human glioblastomas is associated with tumor progression during temozolomide treatment. *Clin Cancer Res* **13**:2038–2045.
- Cai J, Chen J, Zhang W, Yang P, Zhang C, Li M *et al* (2015) Loss of ATRX, associated with DNA methylation pattern of chromosome end, impacted biological behaviors of astrocytic tumors. *Oncotarget* **6**:18105–18115.
- Campbell BB, Light N, Fabrizio D, Zatzman M, Fuligni F, de Borja R *et al* (2017) Comprehensive Analysis of Hypermutation in Human Cancer. *Cell* **171**:1042–1056.e10.
- Cancer Genome Atlas Research Network (2008) Comprehensive genomic characterization defines human glioblastoma genes and core pathways. *Nature* **455**:1061–1068.
- Chamdine O, Gajjar A (2014) Molecular characteristics of pediatric high-grade gliomas. *CNS Oncol* **3**:433–443.
- Cibulskis K, Lawrence MS, Carter SL, Sivachenko A, Jaffe D, Sougnez C *et al* (2013) Sensitive detection of somatic point mutations in impure and heterogeneous cancer samples. *Nat Biotechnol* **31**:213–219.
- Dong SM, Pang JC, Poon WS, Hu J, To KF, Chang AR *et al* (2001) Concurrent hypermethylation of multiple genes is associated with grade of oligodendroglial tumors. *J Neuropathol Exp Neurol* **60**:808–816.
- D'Souza B, Miyamoto A, Weinmaster G (2008) The many facets of Notch ligands. *Oncogene* **27**:5148–5167.
- Fontebasso AM, Schwartzentruber J, Khuong-Quang DA, Liu XY, Sturm D, Korshunov A *et al* (2013) Mutations in SETD2 and genes affecting histone H3K36 methylation target hemispheric high-grade gliomas. *Acta Neuropathol* **125**:659–669.
- Gibbons RJ, McDowell TL, Raman S, O'Rourke DM, Garrick D, Ayyub H *et al* (2000) Mutations in ATRX, encoding a SWI/SNF-like protein, cause diverse changes in the pattern of DNA methylation. *Nat Genet* **24**:368–371.
- Govindan R, Ding L, Griffith M, Subramanian J, Dees ND, Kanchi KL *et al* (2012) Genomic landscape of non-small cell lung cancer in smokers and never-smokers. *Cell* **150**:1121–1134.
- Herwig R, Hardt C, Lienhard M, Kamburov A (2016) Analyzing and interpreting genome data at the network level with ConsensusPathDB. *Nat Protoc* **11**:1889–1907.
- Hoadley KA, Yau C, Hinoue T, Wolf DM, Lazar AJ, Drill E *et al* (2018) Cell-of-origin patterns dominate the molecular classification of 10,000 tumors from 33 types of cancer. *Cell* **173**:291–304.e6.
- Hunter C, Smith R, Cahill DP, Stephens P, Stevens C, Teague J *et al* (2006) A hypermutation phenotype and somatic MSH6 mutations in recurrent human malignant gliomas after alkylator chemotherapy. *Cancer Res* **66**:3987–3991.
- Ichimura K, Bolin MB, Goike HM, Schmidt EE, Moshref A, Collins VP (2000) Deregulation of the p14ARF/MDM2/p53 pathway is a prerequisite for human astrocytic gliomas with G1-S transition control gene abnormalities. *Cancer Res* **60**:417–424.
- Jones PA, Baylin SB (2007) The epigenomics of cancer. *Cell* **128**:683–692.
- Kang H, Tan M, Bishop JA, Jones S, Sausen M, Ha PK *et al* (2017) Whole-Exome Sequencing of Salivary Gland Mucoepidermoid Carcinoma. *Clin Cancer Res* **23**:283–288.
- Karsy M, Gelbman M, Shah P, Balumbu O, Moy F, Arslan E (2012) Established and emerging variants of glioblastoma multiforme: review of morphological and molecular features. *Folia Neuropathol* **50**:301–321.
- Karsy M, Guan J, Cohen AL, Jensen RL, Colman H (2017) New molecular considerations for Glioma: IDH, ATRX, BRAF, TERT, H3 K27M. *Curr Neurol Neurosci Rep* **17**:19.
- Kozak KR, Moody JS (2009) Giant cell glioblastoma: a glioblastoma subtype with distinct epidemiology and superior prognosis. *Neuro Oncol* **11**:833–841.
- Leske H, Brandal P, Rushing EJ, Niehusmann P (2017) IDH-mutant giant cell glioblastoma: A neglected tumor variant? *Clin Neuropathol* **36**:293–295.
- Li J, Duns G, Westers H, Sijmons R, van den Berg A, Kok K (2016) SETD2: an epigenetic modifier with tumor suppressor functionality. *Oncotarget* **7**:50719–50734.
- Li KK, Qi Y, Xia T, Chan AK, Zhang ZY, Aibaidula A *et al* (2017) The kinesin KIF14 is overexpressed in medulloblastoma and downregulation of KIF14 suppressed tumor proliferation and induced apoptosis. *Lab Invest* **97**:946–961.
- Lohkamp LN, Schinz M, Gehlhaar C, Guse K, Thomale UW, Vajkoczy P *et al* (2016) MGMT promoter methylation and BRAF V600E mutations are helpful markers to discriminate pleomorphic xanthoastrocytoma from giant cell glioblastoma. *PLoS One* **11**:e0156422.
- Martincorena I, Campbell PJ (2015) Somatic mutation in cancer and normal cells. *Science* **349**:1483–1489.
- Martinez R, Roggendorf W, Baretton G, Klein R, Toedt G, Lichter P *et al* (2007) Cytogenetic and molecular genetic analyses of giant cell glioblastoma multiforme reveal distinct profiles in giant cell and non-giant cell subpopulations. *Cancer Genet Cytogenet* **175**:26–34.
- Martinez-Diaz H, Kleinschmidt-DeMasters BK, Powell SZ, Yachnis AT (2003) Giant cell glioblastoma and pleomorphic

- xanthoastrocytoma show different immunohistochemical profiles for neuronal antigens and p53 but share reactivity for class III beta-tubulin. *Arch Pathol Lab Med* **127**:1187–1191.
32. Meyer-Puttlitz B, Hayashi Y, Waha A, Rollbrocker B, Boström J, Wiestler OD *et al* (1997) Molecular genetic analysis of giant cell glioblastomas. *Am J Pathol* **151**:853–857.
 33. Müller W, Slowik F, Firsching R, Afra D, Sanker P (1987) Contribution to the problem of giant cell astrocytomas. *Neurosurg Rev* **10**:213–219.
 34. Oh JE, Ohta T, Nonoguchi N, Satomi K, Capper D, Pierscianek D *et al* (2016) Genetic Alterations in Gliosarcoma and Giant Cell Glioblastoma. *Brain Pathol* **26**:517–522.
 35. Oh T, Rutkowski MJ, Safaee M, Sun MZ, Sayegh ET, Bloch O *et al* (2014) Survival outcomes of giant cell glioblastoma: institutional experience in the management of 20 patients. *J Clin Neurosci* **21**:2129–2134.
 36. Ohgaki H (2005) Genetic pathways to glioblastomas. *Neuropathology* **25**:1–7.
 37. Ohgaki H, Kleihues P, Plate KH, Nakazato Y, Bignes DD (2016) Giant cell glioblastoma. In: WHO Classification of Tumours of the Central Nervous System, 4th edn. DN Louis, H Ohgaki, OD Wiestler, WK Cavenee (eds), pp. 46–47. IARC Press: Lyon.
 38. Ortega A, Nuño M, Walia S, Mukherjee D, Black KL, Patil CG (2014) Treatment and survival of patients harboring histological variants of glioblastoma. *J Clin Neurosci* **21**:1709–1713.
 39. Peraud A, Watanabe K, Schwechheimer K, Yonekawa Y, Kleihues P, Ohgaki H (1999) Genetic profile of the giant cell glioblastoma. *Lab Invest* **79**:123–129.
 40. Perry NA, Ackermann MA, Shriver M, Hu LY, Kontogianni-Konstantopoulos A (2013) Obscurins: unassuming giants enter the spotlight. *IUBMB Life* **65**:479–486.
 41. Robinson D, Van Allen EM, Wu YM, Schultz N, Lonigro RJ, Mosquera JM *et al* (2015) Integrative clinical genomics of advanced prostate cancer. *Cell* **161**:1215–1228.
 42. Sabel M, Reifenberger J, Weber RG, Reifenberger G, Schmitt HP (2001) Long-term survival of a patient with giant cell glioblastoma. Case report. *J Neurosurg* **94**:605–611.
 43. Saunders CT, Wong WS, Swamy S, Becq J, Murray LJ, Cheetham RK (2012) Strelka: accurate somatic small-variant calling from sequenced tumor-normal sample pairs. *Bioinformatics* **28**:1811–1817.
 44. Shabihkhani M, Telesca D, Movassaghi M, Naeini YB, Naeini KM, Hojat SA *et al* (2017) Incidence, survival, pathology, and genetics of adult Latino Americans with glioblastoma. *J Neurooncol* **132**:351–358.
 45. Shlien A, Campbell BB, de Borja R, Alexandrov LB, Merico D, Wedge D *et al* (2015) Combined hereditary and somatic mutations of replication error repair genes result in rapid onset of ultra-hypermutated cancers. *Nat Genet* **47**:257–262.
 46. Shriver M, Stroka KM, Vitolo MI, Martin S, Huso DL, Konstantopoulos K *et al* (2015) Loss of giant obscurins from breast epithelium promotes epithelial-to-mesenchymal transition, tumorigenicity and metastasis. *Oncogene* **34**:4248–4259.
 47. Sjoblom T, Jones S, Wood LD, Parsons DW, Lin J, Barber TD *et al* (2006) The consensus coding sequences of human breast and colorectal cancers. *Science* **314**:268–274.
 48. Sun X, Wei J, Wu X, Hu M, Wang L, Wang H *et al* (2005) Identification and characterization of a novel human histone H3 lysine 36-specific methyltransferase. *J Biol Chem* **280**:35261–35271.
 49. Talevich E, Shain AH, Botton T, Bastian BC (2016) CNVkit: Genome-Wide Copy Number Detection and Visualization from Targeted DNA Sequencing. *PLoS Comput Biol* **12**:e1004873.
 50. Tamborero D, Gonzalez-Perez A, Perez-Llamas C, Deu-Pons J, Kandoth C, Reimand J *et al* (2013) Comprehensive identification of mutational cancer driver genes across 12 tumor types. *Sci Rep* **3**:2650.
 51. Viaene AN, Santi M, Rosenbaum J, Li MM, Surrey LF, Nasrallah MP (2018) SETD2 mutations in primary central nervous system tumors. *Acta Neuropathol Commun* **6**:123.
 52. Wang K, Li M, Hakonarson H (2010) ANNOVAR: functional annotation of genetic variants from high-throughput sequencing data. *Nucleic Acids Res* **38**:e164.
 53. Weinstein JN, Akbani R, Broom BM, Wang W, Verhaak RG, McConkey D *et al* (2014) Comprehensive molecular characterization of urothelial bladder carcinoma. *Nature* **507**:315–322.
 54. Wolff RK, Hoffman MD, Wolff EC, Herrick JS, Sakoda LC, Samowitz WS *et al* (2018) Mutation analysis of adenomas and carcinomas of the colon: Early and late drivers. *Genes Chromosomes Cancer* **57**:366–376.
 55. Wu G, Diaz AK, Paugh BS, Rankin SL, Ju B, Li Y *et al* (2014) The genomic landscape of diffuse intrinsic pontine glioma and pediatric non-brainstem high-grade glioma. *Nat Genet* **46**:444–450.
 56. Yan H, Parsons DW, Jin G, McLendon R, Rasheed BA, Yuan W *et al* (2009) IDH1 and IDH2 mutations in gliomas. *N Engl J Med* **360**:765–773.
 57. Yip S, Miao J, Cahill DP, Iafrate AJ, Aldape K, Nutt CL *et al* (2009) MSH6 mutations arise in glioblastomas during temozolomide therapy and mediate temozolomide resistance. *Clin Cancer Res* **15**:4622–4629.
 58. Yu X, Lin Y, Sui W, Zou Y, Lv Z (2017) Analysis of distinct long noncoding RNA transcriptional fingerprints in pancreatic ductal adenocarcinoma. *Cancer Med* **6**:673–680.

SUPPORTING INFORMATION

Additional supporting information may be found in the online version of this article at the publisher's web site:

Figure S1. H&E stained sections of 10 gcGBM samples at (A–J) low and (K–T) high powers.

Figure S2. Representative images of immunohistochemistry staining for H3K36me3 in gcGBM.

Table S1. List of the detected mutations in gcGBM samples.